Hindawi
Advances in Materials Science and Engineering
Volume 2023, Article ID 4414502, 9 pages
https://doi.org/10.1155/2023/4414502

Research Article

Forging Temperature Effects on Crack Tip Creep Behaviour of Hot Hammer Forged Ti-6Al-4V Alloy

Xiurong Fang,[1] **Yan Liu**,[1] **Yanru Shao**,[2] **Huihui Xu**,[1] **and Fuqiang Yang**[1]

[1]*School of Mechanical Engineering, Xi'an University of Science and Technology, Xi'an, China*
[2]*Kangni Mechanical & Electrical Co. Ltd., Nanjing, China*

Correspondence should be addressed to Xiurong Fang; fangxr098@163.com

Received 3 August 2022; Revised 4 November 2022; Accepted 24 November 2022; Published 23 January 2023

Academic Editor: Sengottuvelu Ramesh

The creep behaviour of hot hammer forged Ti-6Al-4V alloy under different forging temperatures has an essential influence on their high-temperature service performance. In this article, the high-temperature mechanical property and creep behaviour of Ti-6Al-4V alloy forging at different forging temperatures were first investigated experimentally. Then, in view of the critical effect of microcracks and other defects on the service life of components in forging, the creep characteristics at the tip of a 2 mm crack were characterized by the finite element method. The results show that when the Ti-6Al-4V alloy was forged at 1000°C, the high-temperature mechanical property was improved, and the steady-state creep rate and creep residual deformation were significantly reduced. In addition, the creep strain and creep rate at the crack tip were decreased apparently during creep, and the creep strain gradient in the crack tip region was also significantly reduced. This indicates that the creep deformation of Ti-6Al-4V alloy can be controlled by an appropriate forging temperature during hot hammer forging process and might delay the crack propagation to improve the service life of components.

1. Introduction

Ti-6Al-4V alloy is used as a structural material for turbine blades because of its high strength, corrosion resistance, and excellent high-temperature properties [1, 2]. The creep behaviour of titanium alloys is critical to blade's service life and the turbine's safety and credibility in high-temperature and pressure service environments [3]. In recent years, to achieve the development goals of ultra-supercritical generating units with high capacity, high power, and long life, the steam temperature and pressure of the turbine were continuously increased, which puts forward a severe test to the creep property of turbine blades [4, 5]. Therefore, the creep behaviour of titanium alloys has received much attention from many researchers. Dvorak et al. [6] performed constant load creep tests on titanium alloy with different annealing temperatures. It was found that titanium prepared at elevated room temperatures had an ultrafine grain size microstructure, which exhibited a higher creep strength than titanium prepared at low temperatures. Dogan et al. [7] studied the effects of microstructure on creep crack growth behaviour of Ti-6242 alloys in the forged and heat-treated condition. The results showed that the material with lamellar microstructure is more creep deformation resistant than the material with equiaxed microstructure. Consequently, the creep behaviour of titanium alloy components is strongly influenced by the preparation process.

The pre-existing microcracks and other defects may exist before the titanium alloy component is put into service. With the increasing of the creep exposure time, the microcracks or other defects inside the material will further grow until the failure of the component [8, 9]. The forging plastic forming process, a common production method for Ti-6Al-4V alloy blades, is applicable to enhance the mechanical properties and can substantially eliminate internal flaws [10]. And compared with hydraulic press forging, the comprehensive mechanical properties of Ti-6Al-4V alloy forged by hot hammer forging are more excellent due to the high deformation rate that leads to the formation of finer grains [2, 11, 12]. Lou et al. [13–15] showed that the variation

of forging parameters during hot hammer forging could significantly affect the phase transformation process of Ti-6Al-4V alloy, in which the variation of forging temperature has a more significant effect on the phase transformation, dislocation motion, and grain boundary slip state during the forging deformation of titanium alloy. It can be clarified that, in the hot hammer forging plastic forming process, the forging temperature is a vital parameter affecting the forging properties.

Creep deformation is induced when titanium alloy components are subjected to long-term operation at high temperature and pressure. The creep deformation accumulation reaches the critical value, the creep crack begins to initiate and propagate, and creep fracture will occur in severe cases [16, 17]. It is effective and accurate to test the creep behaviour of cracks in high-temperature materials using standard specimens. However, the method is time-consuming and highly expensive. Thus, the finite element method is widely used to investigate crack propagation in high-temperature materials. Zhang et al. [18–20] determined the creep damage model based on the material properties of high-temperature alloys, the loading state of the component in service, and investigated the creep crack propagation behaviour by the finite element method. The final physical experiment verified that the simulated data agreed well with the experimental results, which indicated that the numerical method can be used to simulate the creep crack propagation behaviour of high-temperature alloys.

In summary, creep behaviour and creep crack extension of titanium alloy have been extensively investigated and discussed in the last decade. However, few studies focused on how to produce titanium alloy forgings with excellent creep property by controlling the forging process parameters. In this article, the effect of different forging temperatures on the creep behaviour of Ti-6Al-4V alloy forgings is investigated by designing the hot hammer forging temperature. The creep characteristic parameters of the crack tip were further analyzed. It aims to understand the relationship between forging temperature and creep behaviour of titanium alloys after hot hammer forging, which also provides a basis for backtracking the forging process parameters by the creep property requirements of the titanium alloy components.

2. Materials and Methods

2.1. Materials. The commercially available Ti-6Al-4V alloy bars with a diameter of 100 mm and a height of 150 mm were produced by ingot metallurgy. They were provided by China Heavy Machinery Research Institute and the nominal chemical compositions are listed in Table 1.

Table 1: Main chemical composition of Ti-6Al-4V alloy.

Element	Al	V	Fe	O	Impurity	Ti
Wt. (%)	6.29	4.03	0.098	0.16	<0.40	Bal.

2.2. Experimental Procedure

2.2.1. Forging Experiments. As we all know, forging is an experience-oriented technology [21]. The Institute has accumulated a great experience in titanium alloy forging experiments over the years. Therefore, the forging experiments were conducted based on the standard of the forging manual and forging experience [22]. The experimental procedure of forging is shown in Figure 1. The free forging electro-hydraulic hammer of CZYQ-120 had been used in the forging experiment. It has a maximum strike stroke of 1200 mm and strike energy of 120 kJ, respectively, and the mass of the hammerhead is 3400 kg. The energy consumption for preheating and the heat loss in the forging process were considered. Before forging, the upper and lower anvils had been preheated at 200 to 300°C according to the requirements of the institute's forging process. The samples were heated in a special heating furnace with a heating rate of 6°C/min. When the temperature reached the preset forging temperature, the samples were held for 120 min to ensure uniform temperature distribution inside and outside the samples. Due to the relatively narrow forging temperature band of titanium alloys, the whole forging process needs to be completed within 20 s as far as possible. The height reduction of the forgings was controlled by setting the height of the limit block. Finally, the forging was cooled to room temperature by air cooling when the reduction in the overall height of the forgings reached 50%.

It is generally known that the temperature is an important factor affecting the performance of the component during processing [23]. Ti-6Al-4V alloy will crystallize to α-phase in low temperature and transform to β-phase in high temperature, thus the forging of Ti-6Al-4V alloy is divided into $\alpha+\beta$ forging ($T = T_\beta - (30\sim60^\circ C)$), near β forging ($T = T_\beta - (10\sim15^\circ C)$), and β forging ($T > T_\beta$). The measured β-transition temperature of the material was about 985°C [24]. The forging experiment scheme was formulated based on the relationship between the forging temperature and β phase transition temperature as shown in Table 2.

2.2.2. High-Temperature Tensile and Creep Tests. Five groups of tensile samples with five samples in each group were cut from each forged sample for high-temperature tensile and creep tests. Then, all these samples were mechanically polished, cleaned, and dried before testing. As shown in Figures 2(a) and 2(b), the geometrical sizes of standard high-temperature tensile and creep test samples were determined based on high-temperature tensile test method for metal materials (GB/T 228.2-2015) and uniaxial tensile creep test method for metallic materials (GB/T 2039-2012).

The high-temperature tensile tests were carried out at 400°C based on the temperature of the service environment of the turbine blades. Before the test, the samples had been loaded into the high-temperature furnace of the INSTRON 5982 tensile testing machine for heating and held for 15 min when the temperature reached 400°C. The tensile speed was 10 mm/min and the tensile strain rate was $6.67 \times 10^{-3}\ s^{-1}$ during the experiment. The creep tests were conducted on the RD-100 electronic axial tensile creep test machine at a temperature of 400°C, stress loading of 484 MPa, and creep

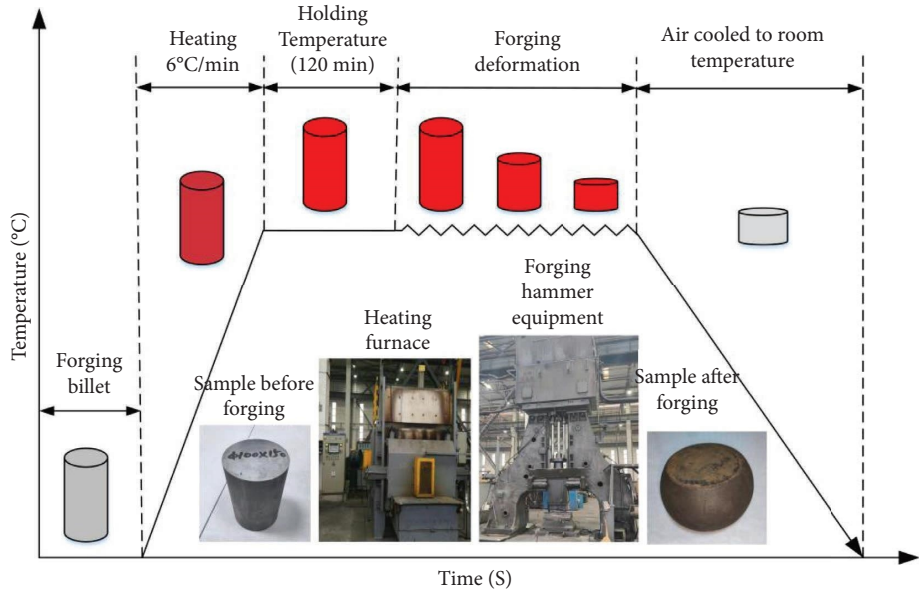

Figure 1: Ti-6Al-4V alloy forging process.

Table 2: Forging experiment scheme of Ti-6Al-4V alloy at different forging temperatures.

Samples	Forging types	Forging temperature (°C)
1#	$\alpha+\beta$	T_β − 60 925
2#	$\alpha+\beta$	T_β − 35 950
3#	Near β	T_β − 10 975
4#	β	T_β + 15 1000
5#	β	T_β + 40 1025

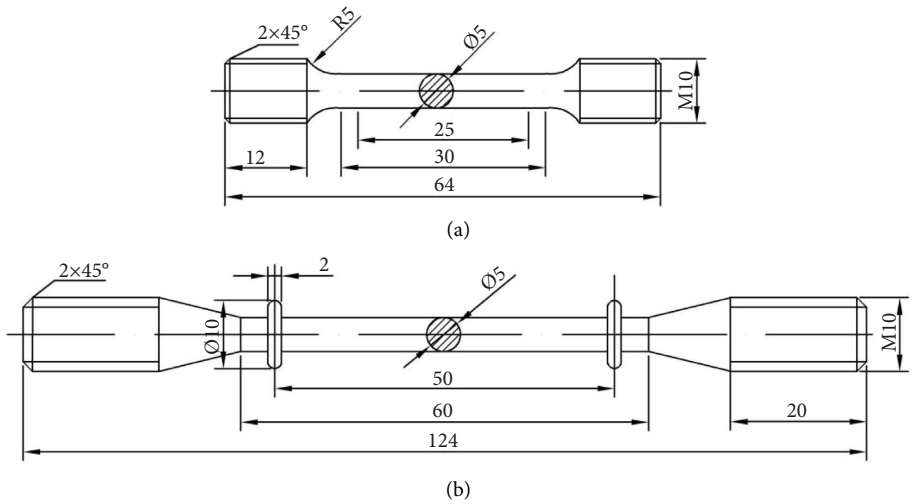

Figure 2: Geometrical sizes of the sample of Ti-6Al-4V alloy (unit: mm): (a) high-temperature tensile sample; (b) creep sample.

time of 80 h. Before testing, the sample had been loaded into the high-temperature furnace for heating and holding for 1 hour when the temperature reached 400°C. The temperature fluctuations were less than ±2°C. Then, the creep stress was loaded with a loading rate of 50 N/s to a preset value and the timing started. The bidirectional extensometer had been

used to measure the creep deformation of the samples and a computerized data acquisition system recorded the creep data in real time.

2.3. Finite Element Method

2.3.1. Constitutive Creep Model. This article studied the creep behaviour of Ti-6Al-4V alloy forging at constant temperature and load, and the time hardening mathematical model is adopted [25, 26]:

$$\dot{\varepsilon} = A\sigma^n t^m, \tag{1}$$

where $\dot{\varepsilon}$ and t are the creep rate and creep time, respectively, A, n, and m are the material constant, stress index, and time index, respectively, A and $n > 0$, and $-1 < m \leq 0$. As shown in equation (2), the expression of creep strain is obtained by integrating equation (1):

$$\varepsilon = \frac{A}{m+1}\sigma^n t^{m+1}, \tag{2}$$

where ε is the creep strain.

2.3.2. Geometry and Mesh Models. The finite element model of the sample with a single-sided crack is shown in Figure 3(a), where W is the width, $2L$ is the length, and the length of the prefabricated crack is a. The constitutive creep model and mechanical property parameters of Ti-6Al-4V alloy at high temperatures were introduced into the CREEP module of ABAQUS. The creep load and creep time were consistent with creep experiments. To balance the calculation efficiency and the accuracy of the results, fine elements were used in the vicinity of the crack tip while coarse elements were used elsewhere. The four-node linear quadrilateral element (CPE4R) was used in the meshing and the global finite element mesh is given in Figure 3(b), and the mesh around the crack tip is shown in Figure 3(c). The geometry of this model was taken as $W = 20$ mm, $L = 25$ mm, and $a = 2$ mm according to the standard SENT sample [27].

3. Results and Discussion

3.1. High-Temperature Mechanical Property. As shown in Figure 4, the averaged mechanical parameters of each sample were calculated after the high-temperature mechanical tensile experiments. When the forging is below the β-phase transition temperature, there is no significant change in the mechanical property of the samples at different forging temperatures. When the forging temperature increases above the β-phase transition temperature to 1000°C, the yield strength and tensile strength are significantly increased with an average increase of 13.8% and 10.6%, respectively. Meanwhile, the reduction of fracture area and elongation also increased by an average of 15.3% and 5.9%. However, when the forging temperature is 1025°C, the comprehensive mechanical property of the sample decreases sharply. This indicates that Ti-6Al-4V alloy forged at a forging temperature of 1000°C has optimum strength and ductility and shows optimal mechanical property.

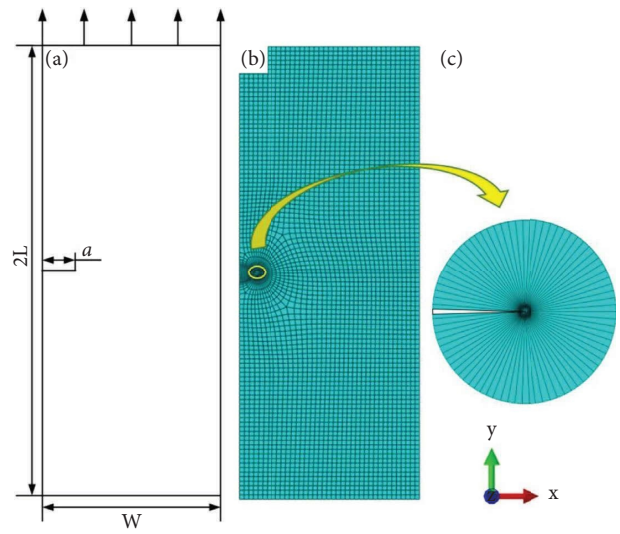

Figure 3: Finite element model: (a) finite element geometry model; (b) global finite element mesh; (c) mesh around the crack tip.

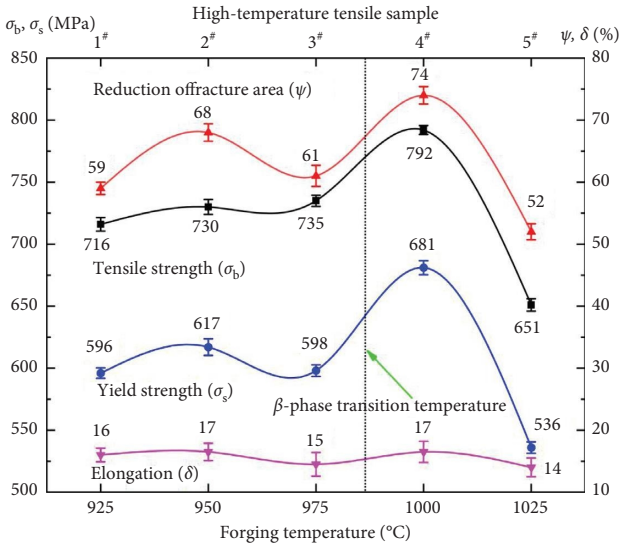

Figure 4: High-temperature mechanical property of Ti-6Al-4V alloy at different forging temperatures (average value of five forged Ti-6Al-4V alloy samples).

3.2. High-Temperature Creep Property. The averaged creep curves of each sample were calculated after the creep experiment, as shown in Figure 5. Creep curves display well-defined two creep stages such as the initial creep stage and steady-state creep stage. When the forging temperature changed, the creep strains of samples 1#, 2#, 3#, and 5# were larger than sample 4# and reached the steady-state creep stage early. This is because, at the forging temperature of 1000°C, the deformation resistance of the forging increases due to the increase in yield strength and ultimate tensile strength; thus, the degree of creep deformation of the forging is reduced.

The majority of creep time is occupied by the steady-state creep stage, and the steady-state creep rate and creep

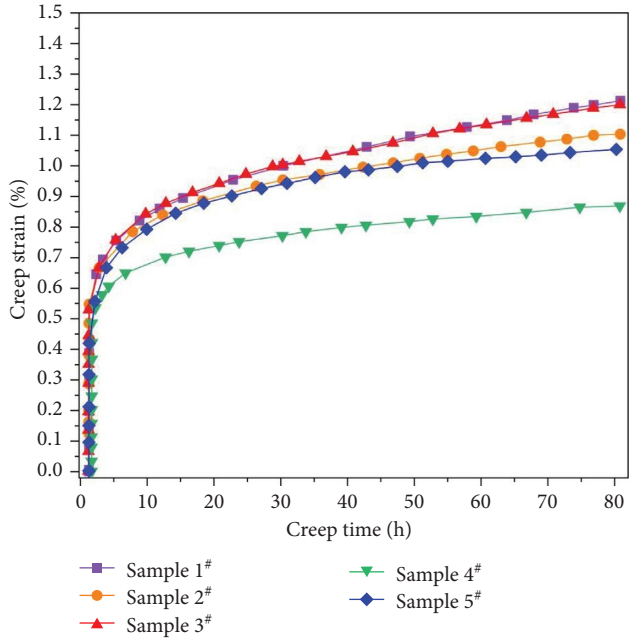

Figure 5: Creep curve of Ti-6Al-4V alloy at different forging temperatures.

residual deformation are usually used to reflect the creep behaviour of the materials [28]. The averaged steady-state creep rate and creep residual deformation of each sample are calculated as shown in Figure 6. With the increase in forging temperature, the steady-state creep rate and creep residual deformation tend to fluctuate downward in general. When the forging temperature is above the β-transition temperature to 1000°C, the steady-state creep rate and creep residual deformation are significantly reduced with an average reduction of 51.3% and 25.6%, respectively. When the forging temperature is 1025°C, the steady creep rate and creep residual deformation increase by another 20% and 30%, respectively. Therefore, during hot hammer forging of Ti-6Al-4V alloy, the creep-induced failure and damage of the forging can be significantly slowed down at a forging temperature of 1000°C. In this way, the service life of the component can be improved.

Studies have shown that the mechanical properties of materials are related to their microstructure. The microstructure of hot hammer forged Ti-6Al-4V at different forging temperatures has been studied by author Fang in the previous work. It was found that the morphology and volume fraction of α and β phases were significantly affected by the forging temperature of hot hammer forging process [2]. As shown in Figures 4–6, when the forging temperature is above the β phase transition temperature to 1000°C, the equiaxed α phase disperses into the $\alpha+\beta$ substrate and the volume fraction of α phase increases. This causes an increase in the forging deformation resistance and a significant improvement in the mechanical property of the forgings. In addition, the lamellar structure is significantly increased, which increases the difficulty of creep slide and hinders the formation of grain boundary voids; the steady-state creep rate and creep residual deformation are reduced after creep. However, with an increasing forging temperature of 1025°C, the α phase nucleates at the grain boundaries and then grows as lamellae into the prior β phase to form the fine needle-like $\alpha+\beta$ lamellar phase, which caused a sharp decrease in the mechanical property of the forgings. Moreover, the numerous $\alpha+\beta$ lamellar phase provides an increasing opportunity for the nucleation of voids, which also aggravates the creep deformation and creep rate of forgings. It can be seen that, with an increasing forging temperature of 1025°C, the creep deformation and creep rate increase the company with a dramatical drop in strength and ductility. Therefore, the finite element analysis of creep was carried out on an alloy forged at 925°C, 950°C, 975°C, and 1000°C, respectively. The critical parameters of the constitutive creep model of equation (2) were fitted according to the experimental creep data, as shown in Table 3.

3.3. The Crack Tip Creep Characteristics

3.3.1. Creep and Creep Rate. The creep curves at the crack tips of the samples is shown in Figure 7(a). During the creep of 80 hours, the creep strain of Ti-6Al-4V alloy at the crack tip under different forging temperatures changed significantly. The creep strain of Ti-6Al-4V alloy forged below β-phase transition temperature is larger than that forged above the β-phase transition temperature. When the creep is carried out for about 70 hours, the creep strain and creep rate of the crack tip gradually stabilizes, and the creep gradually reaches the steady-state creep stage. The minimum creep strain increment at the crack tip of sample 4# is 0.45%, which is reduced by 45.4%, 26.8%, and 42.3% compared to samples 1#, 2#, and 3#, respectively. In addition, as shown in Figure 7(b), sample 4# keeps a low creep rate in the creep process, which not only slows down the creep deformation of the crack tip but also can effectively delay the creep crack propagation. Therefore, at the forging temperature of

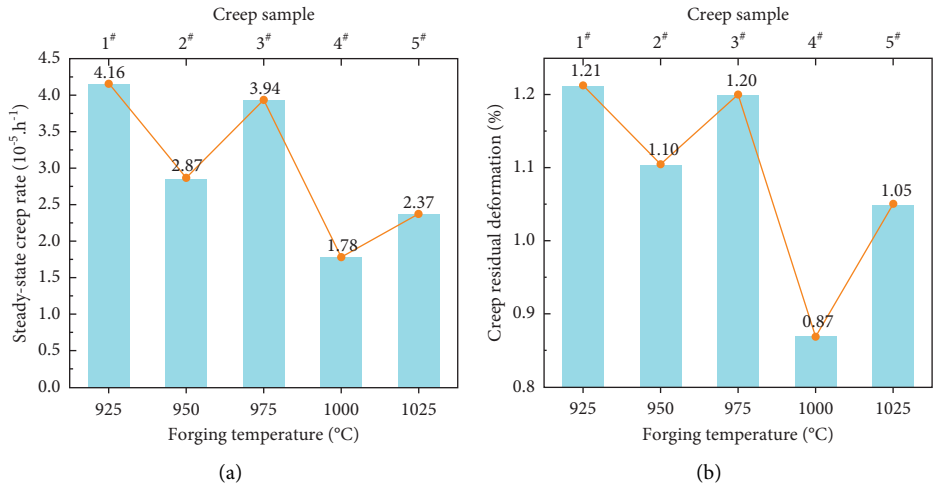

Figure 6: Creep characteristics of Ti-6Al-4V alloy at different forging temperatures: (a) steady-state creep rate; (b) creep residual deformation.

Table 3: Creep equation and parameters of Ti-6Al-4V alloy at different forging temperatures.

Samples	A	n	m
$1^{\#}$	1.7549×10^{-10}	2.5173	−0.8038
$2^{\#}$	3.0787×10^{-9}	2.0278	−0.8509
$3^{\#}$	4.2437×10^{-11}	2.7431	−0.8187
$4^{\#}$	1.1275×10^{-8}	1.7650	−0.8794

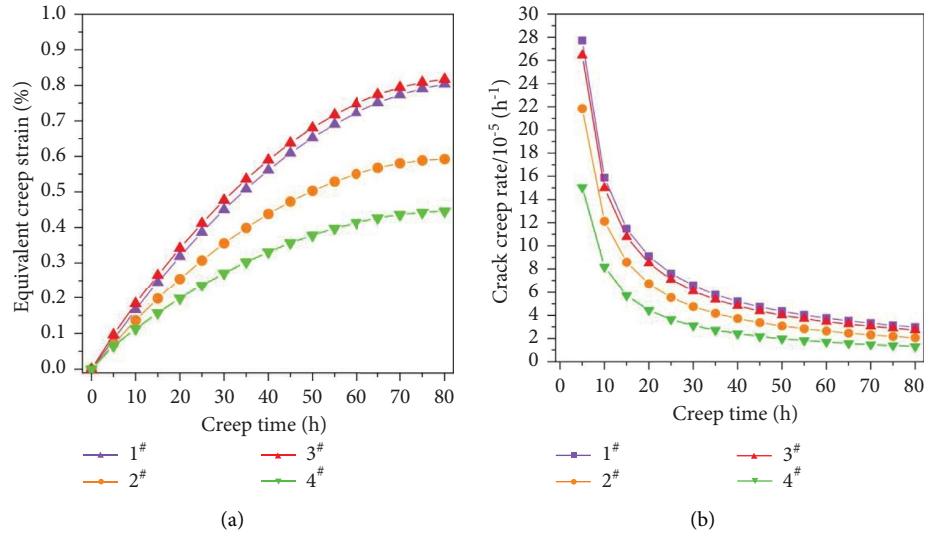

Figure 7: Creep characteristics at the crack tip of Ti-6Al-4V alloy at different forging temperatures: (a) creep curve; (b) creep rate.

1000°C, the creep resistance at the crack tip of the Ti-6Al-4V alloy is significantly improved, which may prolong the service life of titanium alloy components by slowing down the crack expansion process.

3.3.2. Equivalent Creep Strains in the Crack Tip Region. A circular area of $\varphi = 50\,\mu$m at the crack tip was taken to observe the creep strain distribution accurately. As shown in Figure 8, the equivalent creep strains are symmetrically distributed along the direction of crack expansion. The equivalent creep strain gradients at the crack tip of samples $1^{\#}$, $2^{\#}$, and $3^{\#}$ are the most obvious, divided into eight regions by seven contours, and the creep strain corresponds to 0.1%, 0.2%, 0.3%, 0.4%, 0.5%, 0.6%, and 0.7%. However, the equivalent creep strain distribution of sample $4^{\#}$ is only divided by contours 0.1%, 0.2%, 0.3%, and 0.4% into five regions. Furthermore, the creep strain gradients in front and

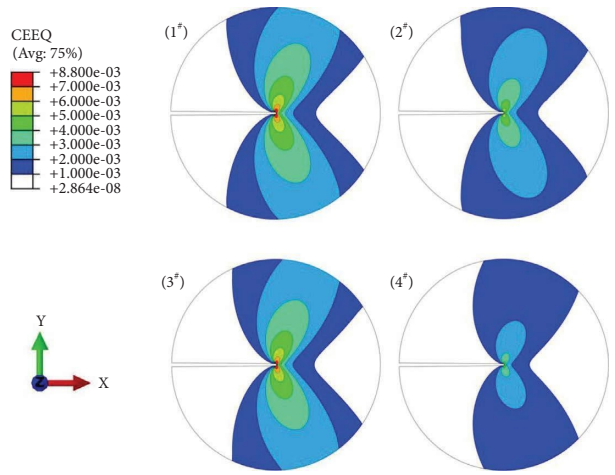

Figure 8: Equivalent creep strain (CEEQ) distribution of Ti-6Al-4V alloy in the crack tip region at different forging temperatures: (1#) 925°C, (2#) 975°C, (3#) 950°C, and (4#) 1000°C.

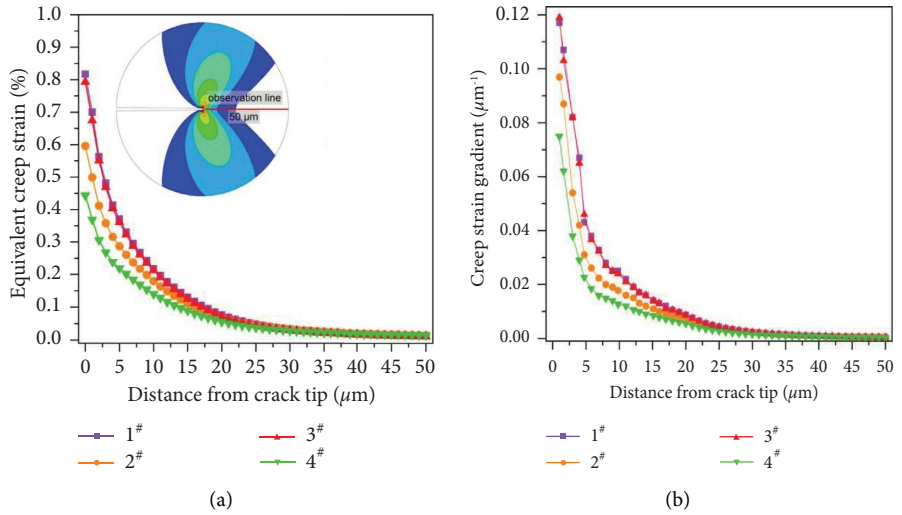

Figure 9: Equivalent creep strain on the observed line in front of the crack tip of Ti-6Al-4V alloy at different forging temperatures. (a) Equivalent creep strain. (b) Creep strain gradient.

on both sides of the crack in samples 1#, 2#, and 3# are larger than those in sample 4#, which indicates that the creep deformation zone is significantly reduced and the equivalent creep strain in the X and Y directions will be a smaller strain gradient in the crack tip region with increasing forging temperature to 1000°C.

The maximum value of mechanical parameters is located in front of the crack propagation. The equivalent creep strain distribution on the 50 μm observation line in front of the crack tip is presented in Figure 9(a). The maximum value of equivalent creep strain at the crack tip decreases sharply and then tends to be flat as the distance from the crack tip increases. The equivalent creep strain values of the 4 samples gradually tend to 0.05% when the distance from the crack tip is beyond 30 μm. It means that the influence of forging temperature on the creep deformation in the crack tip region of the Ti-6Al-4V alloy forging is weakened with the increase of the distance from the crack tip. Moreover, as shown in Table 4, sample 4# exhibits the minimum reduction in equivalent creep strain on the observation line, which decreased by 48.1%, 27.3%, and 46.7%, respectively, compared to samples 1#, 2#, and 3#.

The driving force of creep crack propagation is determined by the creep strain gradient, and it is reasonable to characterize the creep crack propagation behaviour with a creep strain gradient [29]. As shown in Figure 9(b), the creep strain gradient of the crack tip of the sample at different forging temperatures shows the same trend as the creep strain. On the line of observation in front of the crack, the creep strain gradient of sample 4# was significantly reduced compared to samples 1#, 2#, and 3#.

It indicates that when the forging temperature is above the β-phase transition temperature to 1000°C, Ti-6Al-4V alloy forging can keep a low creep strain and creep strain gradient in the crack tip region during the creep process even if there is the appearance of microcracks. The low creep

Table 4: Comparison of equivalent creep strains on observation lines of Ti-6Al-4V alloy at different forging temperatures.

Samples	Maximum equivalent creep strain (%)	Minimum equivalent creep strain (%)	Reduction (%)
$1^{\#}$	0.82	0.05	0.77
$2^{\#}$	0.60	0.04	0.56
$3^{\#}$	0.80	0.05	0.75
$4^{\#}$	0.45	0.05	0.40

strain gradient means that the driving force of crack propagation will be reduced. Therefore, the crack propagation rate will also be effectively slowed down during the service of the components, which is important for improving the service life of Ti-6Al-4V alloy forging.

4. Conclusions

From a sustainability viewpoint, the creep behaviour and creep characteristics at the crack tip of the forged Ti-6Al-4V alloy were investigated by physical experiments. Then, the creep characteristics of the crack tip with the same crack length were analyzed by a finite element method according to the experimental data.

The experimental results show that the forgings forged at 1000°C exhibited optimum high-temperature mechanical and creep property. The yield strength and tensile strength increased by an average of 14.2% and 10.6%, respectively, while the elongation and section shrinkage improved by an average of 15.3% and 5.9%, respectively. In addition, steady-state creep rate and creep residual deformation decreased with an average of 51.3% and 25.6%, respectively.

It was found by the finite element method that Ti-6Al-4V alloy forged at the temperature of 1000°C was creeping for 80 hours, the forging has the minimum creep strain with 0.45%, and it kept the lowest creep rate at the crack tip. Moreover, the creep deformation zone was significantly reduced, and the equivalent creep strain in the X and Y directions will be a smaller strain gradient in the crack tip region. Especially, in the observation line in front of the crack tip, the creep strain was reduced by 0.4% and kept the minimum value, which resulted in a significant reduction of the creep strain gradient and effectively delayed the crack extension.

It also indicated that, in the hot hammer forging process, appropriate forging process parameters such as forging temperature for Ti-6Al-4V alloy can be designed to help reduce the creep deformation, which can effectively improve the service life and reliability of Ti-6Al-4V alloy components as well as lower the billet waste and maintain minimum energy consumption for forging production.

Data Availability

The data used to support the findings of this study are included within the article.

Conflicts of Interest

The authors declare that they have no conflicts of interest.

Acknowledgments

This work was funded by the National Natural Science Foundation of China (Grant nos. 52175145 and 51775427).

References

[1] S. Ramesh, K. Palanikumar, S. B. Boppana, and E. Natarajan, "Analysis of chip formation and temperature measurement in machining of titanium alloy (Ti-6Al-4V)," *Experimental Techniques*, vol. 48, 2022.

[2] X. R. Fang, L. Liu, J. Lu, and Y. Gao, "Optimization of forging process parameters and prediction model of residual stress of Ti-6Al-4V alloy," *Advances in Materials Science and Engineering*, vol. 2021, Article ID 3105470, 2021.

[3] W. Choi, H. Yoon, and B. D. Youn, "Operation-adaptive damage assessment of steam turbines using a nonlinear creep-fatigue interaction model," *IEEE Access*, vol. 8, pp. 126776–126783, 2020.

[4] H. He, Z. B. Zheng, Z. J. Yang, X. Wang, and Y. Wu, "Failure analysis of steam turbine blade roots," *Engineering Failure Analysis*, vol. 115, no. 4, pp. 104629–111281, 2020.

[5] Y. Sun and B. Xu, "On real-time creep damage prediction for steam turbine," *Transactions of the Institute of Measurement and Control*, vol. 44, no. 13, pp. 2603–2610, 2022.

[6] J. Dvorak, P. Kral, A. G. Kadomtsev et al., "Influence of cryo-processing and post-SPD annealing on creep behavior of CP titanium," *Materials*, vol. 15, no. 5, pp. 1646–1653, 2022.

[7] B. Dogan, A. Saxena, and K. H. Schwalbe, "Creep crack growth in creep-brittle Ti-6242 alloys," *Materials at High Temperatures*, vol. 10, no. 2, pp. 138–143, 2016.

[8] Y. C. Wang, X. Y. Xue, H. C. Kou et al., "Quasi-in-situ investigation on microstructure degradation of a fully lamellar TiAl alloy during creep," *Journal of Materials Research and Technology*, vol. 18, pp. 4980–4989, 2022.

[9] I. P. Semenova, K. S. Selivanov, R. R. Valiev et al., "Enhanced creep resistance of an Ultrafine-Grained Ti–6Al–4V alloy with Modified surface by Ion Implantation and (Ti + V)N coating," *Advanced Engineering Materials*, vol. 22, no. 10, pp. 1901219–1901247, 2020.

[10] N. M. Prabu, S. Nallusamy, and G. Sureshkannan, "Investigation of heat transfer enhancement effect on normal and nano coated wick structure heat pipes-A comparative assessment," *International Journal of Engineering Research in Africa*, vol. 51, pp. 191–198, 2020.

[11] J. Cai, M. Guo, P. Peng et al., "Research on hot deformation behavior of as-Forged TC17 titanium alloy," *Journal of Materials Engineering and Performance*, vol. 30, no. 10, pp. 7259–7274, 2021.

[12] G. Sureshkannan, V. Thangarasu, N. Manikanda Prabu, and D. Anburose, "Review on extrusion of magnesium matrix nano composites," *International Journal of Nano-manufacturing*, vol. 14, no. 1, pp. 1–342, 2018.

[13] S. Y. Luo, J. N. Yao, J. Li, H. Du, H. Liu, and F. Yu, "Influence of forging velocity on temperature and phases of

forged Ti-6Al-4V turbine bladefluence of forging velocity on temperature and phases of forged Ti-6Al-4V turbine blade," *Journal of Materials Research and Technology*, vol. 9, no. 6, pp. 12043–12051, 2020.

[14] Q. Ma, K. Wei, Y. Xu, L. Zhao, and X. Zhang, "Exploration of the static softening behavior and dislocation density evolution of TA15 titanium alloy during double-pass hot compression deformation," *Journal of Materials Research and Technology*, vol. 18, pp. 872–881, 2022.

[15] T. R. Prabhu, "Simulations and experiments of the nonisothermal forging process of a Ti-6Al-4V impeller," *Journal of Materials Engineering and Performance*, vol. 25, no. 9, pp. 3627–3637, 2016.

[16] P. Aliprandi, F. Giudice, E. Guglielmino, and A. Sili, "Tensile and creep properties improvement of Ti-6Al-4V alloy specimens produced by electron beam powder bed fusion additive manufacturing," *Metals*, vol. 9, no. 11, pp. 1207–1436, 2019.

[17] W. Zhang, X. W. Wang, H. F. Chen, T. Y. Zhang, and J. M. Gong, "Evaluation of the effect of various prior creep-fatigue interaction damages on subsequent tensile and creep properties of 9%Cr steel," *International Journal of Fatigue*, vol. 125, pp. 440–453, 2019.

[18] Y. C. Zhang, W. C. Jiang, S. T. Tu, X. C. Zhang, Y. J. Ye, and R. Z. Wang, "Experimental investigation and numerical prediction on creep crack growth behavior of the solution treated Inconel 625 superalloy," *Engineering Fracture Mechanics*, vol. 199, pp. 327–342, 2018.

[19] D. Q. Wu, L. Y. Xu, W. Zhai, H. Jing, L. Zhao, and Y. Han, "Analysis of the constraint levels and the creep crack initiation times for pressurized pipes with long surface cracks," *Thin-Walled Structures*, vol. 153, Article ID 106787, 2020.

[20] R. Okamoto, S. Suzuki, M. Sakaguchi, and H. Inoue, "Evolution of short-term creep strain field near fatigue crack in single crystal Ni-based superalloy measured by digital image correlation," *International Journal of Fatigue*, vol. 162, Article ID 106952, 2022.

[21] T. Altan, G. Ngaile, and G. Shen, *Cold and hot Forging: Fundamentals and Applications*, ASM International, Almere, Netherlands, 2005.

[22] Society of Plasticity Engineering, "Chinese mechanical Engineering Society, forging manual - forging workshop equipment," *Machinery Industry, Ver.*,vol. 3, 2013.

[23] R. Viswanathan, S. Ramesh, and N. Elango, "Temperature measurement and optimisation in machining magnesium alloy using RSM and ANOVA," *Pertanika J. Sci. Technol*, vol. 25, no. 1, pp. 255–262, 2017.

[24] J. S. Jha, S. P. Toppo, R. Singh, A. Tewari, and S. K. Mishra, "Understanding flow behavior and microstructure evolution during thermomechanical processing of mill-annealed Ti-6Al-4V titanium alloy," *Matls. Perf. Charact*, vol. 8, no. 5, pp. 20190010–20190021, 2019.

[25] H. Y. Jing, D. B. Su, L. Y. Xu et al., "Finite element simulation of creep-fatigue crack growth behavior for P91 steel at 625°C considering creep-fatigue interaction," *International Journal of Fatigue*, vol. 98, pp. 41–52, 2017.

[26] W. M. Ye, X. T. Hu, and Y. D. Song, "A new creep model and its application in the evaluation of creep properties of a titanium alloy at 500 °C," *Journal of Mechanical Science and Technology*, vol. 34, no. 6, pp. 2317–2326, 2020.

[27] Y. F. Huang and W. X. Zhou, "Stress intensity factor for clamped SENT specimen containing non-straight crack front and side grooves," *Theoretical and Applied Fracture Mechanics*, vol. 93, pp. 116–127, 2018.

[28] Z. Z. Zheng, F. T. Kong, Y. Y. Chen, and X. P. Wang, "Effect of nano-Y2O3 addition on the creep behavior of an as-cast near-α titanium alloy," *Materials Characterization*, vol. 178, pp. 111249–249, 2021.

[29] Y. Liu and S. Cai, "Gradients of strain to increase strength and ductility of magnesium alloys," *Metals*, vol. 9, no. 10, pp. 1028–1036, 2019.